EXCITATION PROPERTIES OF THE SQUID AXON MEMBRANE AND MODEL SYSTEMS WITH CURRENT STIMULATION

STATISTICAL EVALUATION AND COMPARISON

JÜRGEN F. FOHLMEISTER, WILLIAM J. ADELMAN, JR., AND RICHARD E. POPPELE,
Laboratory of Biophysics, Intramural Research Program, National Institute of Neurological and Communicative Disorders and Stroke, National Institutes of Health at the Marine Biological Laboratory, Woods Hole, Massachusetts 02543 and Laboratory of Neurophysiology, University of Minnesota, Minneapolis, Minnesota 55455 U.S.A.

ABSTRACT The space-clamped squid axon membrane and two versions of the Hodgkin-Huxley model (the original, and a strongly adapting version) are subjected to a first order dynamic analysis. Stable, repetitive firing is induced by phase-locking nerve impulses to sinusoidal currents. The entrained impulses are then pulse position modulated by additional, small amplitude perturbation sinusoidal currents with respect to which the frequency response of impulse density functions are measured. (Impulse density is defined as the number of impulses per unit time of an ensemble of membranes with each membrane subject to the same stimulus.) Two categories of dynamic response are observed: one shows clear indications of a corner frequency, the other has the corner frequency obscured by dynamics associated with first order conductance perturbations in the interspike interval. The axon membrane responds with first order perturbations whereas the unmodified Hodgkin-Huxley model does not. Quantitative dynamic signatures suggest that the relaxation times of axonal recovery excitation variables are twice as long as those of the corresponding model variables. A number of other quantitative differences between axon and models, including the values of threshold stimuli are also observed.

INTRODUCTION

When the membrane of the squid giant axon is electrically "space-clamped" in an experimental chamber, and stimulated with a depolarizing current of either step or ramp time-course, its electrical response, at first sight, is quite simple to describe. For a step magnitude or ramp slope smaller than a certain critical value ($\sim$ 10 $\mu A/cm^2$ and 2.5 $\mu A/cm^2/ms$, respectively), the axons respond. with strongly damped, subthreshold membrane potential oscillations. Above the critical (threshold) values, the axons respond with a single action potential with a latency that is inversely related to the stimulus magnitude, and is never more than $\sim$ 6 ms at 6.3°C (unpublished observation; however, other investigators have seen trains of impulses of various durations in response to suprathreshold current steps, e.g., Hagiwara and Oomura, 1958; Best, 1979, Fig. 3). The Hodgkin-Huxley (1952) model describes reasonably well the latency and action potential wave-form for simulated stimulus magnitudes that are suprathreshold for the squid axon. (This condition must be added because any nonzero ramp slope

is suprathreshold for the model, which does not accommodate completely and always begins to fire repetitively, albeit with very long latency for ramps with very small slopes.) The model however fires continuously for all suprathreshold step and ramp stimuli with the exception of a very narrow range of current steps in the vicinity of threshold for which the model responds with one or two impulses.

There have been a number of attempts to reconcile model behavior with the squid axon (e.g., Adelman and Fitzhugh, 1975; Fohlmeister, 1975; c.f. also Jakobsson, 1978, for further references). Although for most of these the new model's adaptation does correspond more or less with the axon, in no case does the membrane potential trajectory following the spike agree with that of the axon. For each of these models the postspike undershoot is overly precipitous and recovery from the undershoot too rapid to agree with the axon's trajectory. Reconciling the adaptive response alone, therefore, is not sufficient for an accurate description of the axon's excitation properties.

As a test for both models and axon, we have therefore chosen to study their dynamic responses to small amplitude sinusoidal signals. A sinusoidal perturbation occurring with a random phase in the interspike interval influences the timing of action potential occurrence in a repetitive train which is in turn established by conductance and other membrane parameters in the intervals. The technique has been applied to neurons which exhibit tonic repetitive firing (Poppele and Chen, 1972; Fohlmeister et al., 1974, 1977*b*), and has yielded membrane conductance parameters as a function of time into the interspike intervals. To apply this technique to adapting systems, the neuron or model must be able to respond with stable repetitive firing to a stimulus current density of the form

$$I(t) = I_0\{1 + a \cdot \sin(2\pi f_0 t)\}, \tag{1}$$

and the simplest response pattern (the one used here) is to establish one impulse per cycle of the sine wave (one-to-one phase locking). This is illustrated in Fig. 1 (cf. also Guttman and Feldman, 1978).

The purpose of the locking signal is to establish an indefinitely long repetitive spike train; tonic neurons may therefore also be tested dynamically without the locking sine wave (see Appendix). The dynamics themselves are measured with the use of perturbing sine wave currents of small amplitude superimposed on the current responsible for the repetitive train. The frequency, f_m, of the perturbing sine wave is one of a set of frequencies each of which is less than the locking frequency, f_0; the set of f_m covers a range of frequencies extending two orders of magnitude below f_0. This second sine wave produces a pulse position modulation of the impulses of the steady-state train generated by the locking sinusoid. Because there is no phase relation between the two stimulus sine waves however, the state of the membrane in successive cycles of perturbation will be different from the states in all other cycles. Analyzing a long, modulated impulse train with continuous perturbation cycles is therefore equivalent to an analysis over a single perturbation cycle of the impulse density response of an ensemble of membranes each with a different initial condition. (Of course some initial conditions are favored over others; this is true for the ensemble as well as the continuous impulse train.) For sufficiently small amplitude perturbations the density of impulses varies sinusoidally with the period of the perturbing sine wave (Fig. 2). The amplitude of this density modulation is plotted as a point of a gain curve. Similarly the phase of this impulse density curve relative to

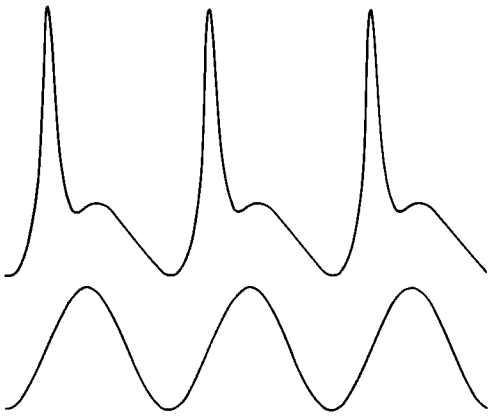

FIGURE 1

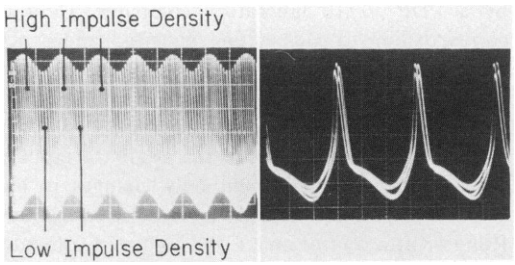

FIGURE 2

FIGURE 1 Model membrane potential trajectory (upper trace) in response to the locking-current density of Eq. 1 with $I_0 = 88\ \mu A/cm^2$, $a = 1.0$, and $f_0 = 75$ Hz (lower trace). Model parameters correspond to those of Adelman and Fitzhugh (1975, Fig. 11) except $T = 6.3°C$.

FIGURE 2 Multiple oscilloscope traces of impulses and interspike membrane-potential trajectories generated by the space-clamped axon membrane in response to the locking current plus 25% modulation. (A) Traces were triggered on sync pulses associated with the modulation sine wave. Note the modulation in impulse density with the period of the perturbation sine wave; the latter is also responsible for the modulation of the postspike undershoots and spike peaks. $I_0 = 79\ \mu A/cm^2$, $f_0 = 75$ Hz, $f_m = 64.9$ Hz, and $T = 6.5°C$. Oscilloscope grid is 20 mV/div vertical and 10 ms/div horizontal scale. (B) Scope traces triggered on impulses. $I_0 = 77\ \mu A/cm^2$, $f_0 = 150$ Hz, $f_m = 22.8$ Hz, and $T = 13°C$. Scale is 20 mV/div vertical and 2 ms/div horizontal.

the phase of the perturbing sine wave is plotted as a point of a phase curve. A pair of gain and phase curves, called a Bode plot, is then used like a template for comparison among models and the axon.

Specific features of the Bode plots (corner frequencies, slope of the gain curves, and phase advance as a function of f_m, etc.) correspond directly to such parameters as magnitude of conductance in the interspike interval for simple models (e.g., the so-called "leaky integrator" models, see Appendix), but require additional interpretation for models as complex as the Hodgkin-Huxley model. For such models and for the axon the dynamics provide a clear descriptive indication of differences during repetitive discharges under normal current stimulation. The Bode plots by themselves however do not show the way to reconcile those differences.

In this report we restrict ourselves to a presentation of axon and model data along with a preliminary analysis of that data. The existing models do not reproduce the dynamics of the axon, and certain of the more direct implications stemming from the differences are discussed.

METHODS

Cleaned, single giant axons from the hindmost stellar nerve of the squid, *Loligo pealei,* were used in this study. Intact axons were externally bathed in artificial seawater (Adelman et al., 1973). The axons were current-clamped by the method described in Binstock et al. (1975) using a sinusoidal current stimulation rather than short duration square wave currents. A locking sinusoidal current of the form given by Eq. 1

with a = 1.0 was adjusted to assure the production of one spike per cycle at f_0 = 100 Hz. (Fig. 1), and typically this required I_0 = 80 μA/cm^2. A second, small amplitude-modulating sinusoidal current (of amplitude $I_0/4$) was linearly summed with the locking current to produce a sinusoidal variation of impulse density over a modulating cycle (Fig. 2). Action potentials produced by the axon and sync pulses marking each cycle of the modulating sinusoid were treated as all-or-none events that were timed on-line by a PDP 11/10 laboratory computer. Data consisted of clock times (to the nearest 0.2 ms) corresponding to each action potential and sync pulse for a total of at least 200 events for each modulating frequency tested. The data were stored on binary magnetic tape for later processing on an IBM 1800 computer (IBM Corp., White Plains, N.Y.). This consisted of estimating impulse density sinusoids and computing gain and phase for Bode plots (Fohlmeister et al., 1977*a*). These functions are defined in the Appendix. For this study the input modulation was held constant (25%) and the "gains" reported therefore represent only changes in output modulation. They were computed as 20 log (modulation amplitude). Model impulse trains were generated by numerical integration using a library Runge-Kutta routine on a CDC Cyber 74 computer and a continuous system modeling program on the IBM 1800 computer. An explanation of the basic technique and interpretations of various Bode signatures are presented in the Appendix.

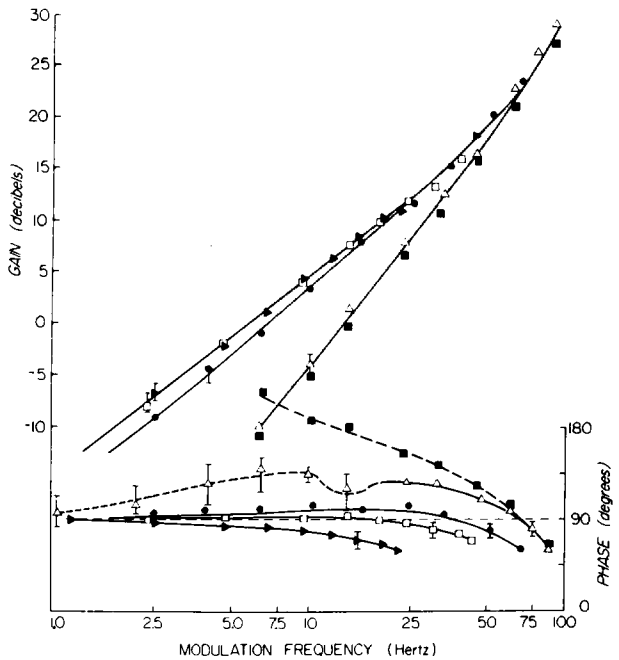

FIGURE 3 Gain (upper set of curves) and phase plots (lower set of curves) of space-clamped squid axon membranes at 6.3°C stimulated as in Eq. 2 with I_0 in the range 72–88 μA/cm^2 and I_1 in the range of 18–22 μA/cm^2 but such that $I_1 = I_0/4$ always. The dip in the phase curve for f_0 = 100 Hz occurring in the neighborhood of f_m = 14 Hz corresponds to an instability at which the phase vacillates among two or more preferrential values. Harmonic distortion is therefore correspondingly high at this frequency and somewhat elevated for all $f_m \lesssim 14$ Hz (dashed curve). Some axons do not show this phase dip and continue a smooth-phase decline towards 90° for lower f_m. Two axons generated a phase which tended towards a 270° advance as $f_m \rightarrow 0$ (upper dashed curve). Such a phase is also generated by a model of the squid axon presented in Fohlmeister (1975) which operates with a relatively large K conductance and exhibits strong adaptation properties. Symbols are representative data from a single axon for f_0 = 100 Hz (△), 75 Hz (●), 50 Hz (□), and 25 Hz (▶). Curves are the gain and phase averaged from nine axons. Error bars indicate the maximum deviation from the mean level shown by any data point used in calculating the mean for all modulation frequencies of a given curve.

RESULTS

Squid Axon Dynamics

At the operating temperature of 6.3°C most healthy axons can be made to phase-lock at the rate of f_0 = 100 impulses/s in response to sinusoidal current density as in Eq. 1 with a = 1.0. The minimum value of I_0 necessary for this response is ~ 75 μA/cm^2. All axons capable of this repetitive rate are also able to maintain one-to-one phase locking for f_0 = 75, 50, 25, and 10 Hz. The minimum required magnitude of I_0 declines steeply with f_0 to a plateau of ~ 30 μA/cm^2 for f_0 below 50 Hz. A majority of the axons continue repetitive firing over the entire range of modulation frequencies (no dropped spikes) when the locking signal (Eq. 1) is modulated by 25%;

$$I(t) = I_0\{1 + \sin(2\pi f_0 t)\} + I_1 \sin(2\pi f_m t + \varphi), \quad (2)$$

where $I_1 = (0.25)I_0$ and φ is an arbitrary phase angle. The resulting Bode plots of Fig. 3 are derived from the data from nine axons.

For very low modulation frequencies, f_m, all phase curves tend to a phase advance of 90° (relative to the perturbation sine wave) with the exception of an occasional axon firing at f_0 = 100 Hz which tends towards a 270° advance. Depending on the firing rate, and in particular for higher f_0, the phase advance increases in the midrange of modulation frequencies, f_m, to reach a maximum somewhere in the area of $10 \lesssim f_m \lesssim 25$ Hz. The phase advance again

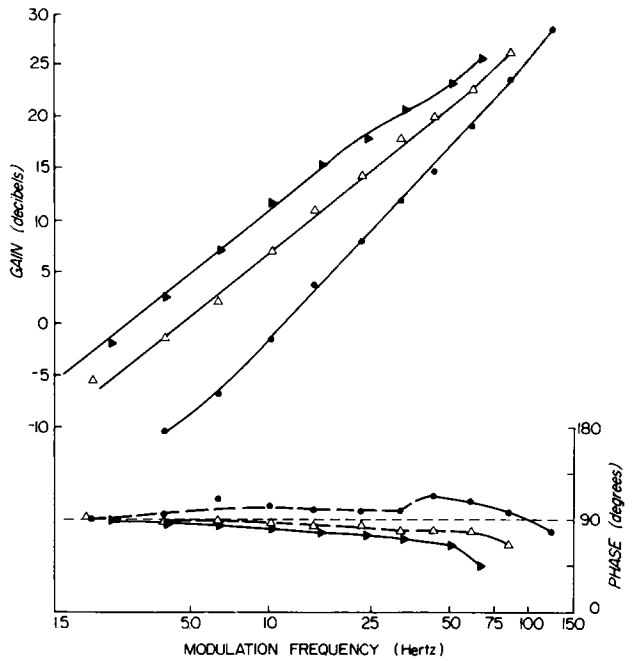

FIGURE 4 Representative data from a single axon. Gain and phase plots of the space-clamped membrane of the squid axon at 13.2°C stimulated as in Eq. 2 with I_0 = 78 μA/cm^2 and I_1 = 19.5 μA/cm^2. Note the general shift in the dynamics to higher locking frequencies, f_0, as compared with the data at 6.3°C (Fig. 3). f_0 = 150 Hz (●), 100 Hz (△), and 75 Hz (▶).

decreases to well below 90° as f_m approaches f_0. The midrange phase advance is invariably accompanied by a direct increase in the slope of the gain curve, which is a constant 6 dB/octave for the lower modulation frequencies.

Further dynamics data of the squid axon were obtained for a wide range of temperatures and found to be strongly temperature-dependent. Representative data from one axon, obtained at 13.2°C, is plotted in Fig. 4. The overall dynamic characteristics appear to simply shift to higher frequencies, f_0 and f_m, for higher temperatures.

The axon is able to maintain a phase-locked impulse rate of 150 impulses/s at 12°C and 200 impulses/s at 18°C. These dynamic response properties are consistent with the strong temperature dependence (Q_{10} = 2.7–3.0) of the rate constants of the excitable conductance channels and indicate that the dynamics are a direct function of the channel kinetics.

Hodgkin-Huxley Model Dynamics

The Hodkin-Huxley (1952) model for the excitation kinetics of the squid axon membrane will phase-lock to the "stimulus current" of Eq. 1 for values of $10 \lesssim I_0 \lesssim 20$ μA/cm^2 in the range of $50 \lesssim f_0 \lesssim 120$ Hz at 6.3°C. Larger values of I_0 continue to produce phase locking and increase the upper bound of f_0 to 200 Hz when I_0 = 75 μA/cm. However, because of the inherent repetitive firing properties of the model (Fig. 5) double spiking begins to occur for the smaller values of f_0 (cf. also Holden, 1976). This is particularly true if one attempts to modulate sinusoidally a one-to-one phase-locked impulse train at even lower frequencies, f_0. For example, at the frequency f_0 = 25 Hz it is possible to maintain the one-to-one condition

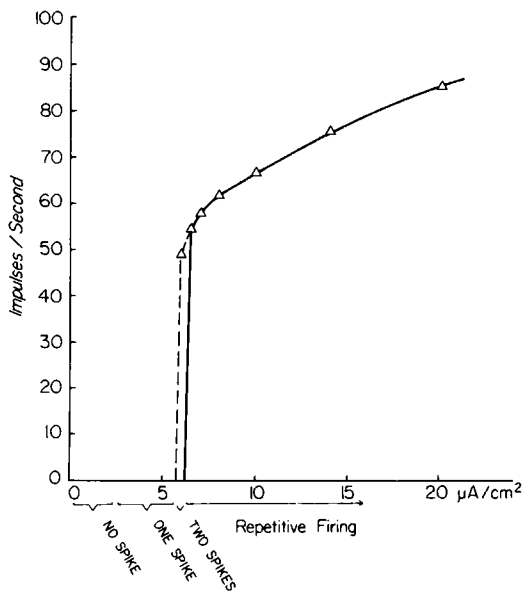

FIGURE 5 Impulse frequency vs. stimulus current density for the Hodgkin-Huxley (1952) model under constant current stimulation at 6.3°C. Note that 55 impulses/s is the practical lower bound of the repetitive firing frequency range. Dashed curve represents the reciprocal of the interspike period between the pair of spikes generated near the onset of the step stimulus in this range. The bracketed ranges of current density (abscissa) are defined by the type of impulse response that is generated after the onset of a step stimulus of that magnitude.

with 20% modulation (I_1 = 0.73 μA/cm^2) and with I_0 = 3.66 μA/cm^2. "Double spiking" and dropped spikes occur when I_0 is changed by ~ 10% from this value, however. Further, the model dynamic response for lower f_0 is qualitatively different from that at the higher locking frequenices (Fig. 6).

The phase curves of the model data again approach a 90° advance for small f_m, but then begin a decline for modulation frequencies in the midrange ($5 \lesssim f_m \lesssim 30$ Hz, cf. Fig. 6) and for $f_0 > 55$ Hz. Simultaneously, the slope of the gain curves begins to decrease from the asymptotic rate of 6 dB/octave as they begin to round the "corner frequency" (defined in Appendix). For the model, the theoretical recognition points for a corner frequency are not fully realized because the dynamic resonance sets in which leads to an additional gain enhancement and phase advance as the modulation frequency, f_m, approaches the impulse frequency f_0. The amount of dynamic interaction between the "corner" and "resonance" phenomena depends both on the separation between the corner frequency and f_0, and on the width of the resonance. Fig. 6 shows that these dynamic phenomena become more clearly separated for higher impulse frequencies, f_0, for the Hodgkin-Huxley model.

The dynamics associated with the resonance are algebraically additive with those of the corner frequency (see Appendix). To determine the resonance alone the dynamics must be measured in the absence of the locking signal. This is possible, and has been done for the Hodgkin-Huxley model, because that model fires repetitively at both 75 and 100 impulses/s under the appropriate level of constant current stimulation (Fig. 5). The corner frequency,

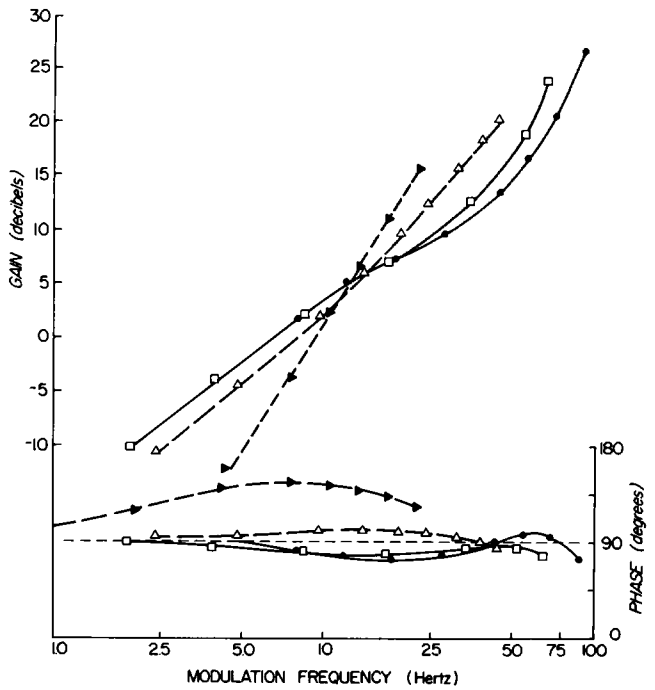

FIGURE 6 Gain and phase plots generated by the Hodgdin-Huxley model at 6.3°C. I_0 = 20 μA/cm^2 for f_0 = 100 Hz (●), 10 μA/cm^2 for 75 (□) and 50 Hz (△), and 3.66 μA/cm^2 for 25 Hz (▶). I_1 = 5 μA/cm^2 for f_0 = 100 Hz, 2.5 μA/cm^2 for 75 and 50 Hz, and 0.73 μA/cm^2 for 25 Hz.

determined by subtracting out the resonance, is found to be 15.5 ± 0.5 Hz at 6.3°C for both of these impulse frequencies.

At the lower locking frequencies $f_0 \leq 55$ Hz the model dynamics change in quality (Fig. 6, dashed curves). In this range—which is outside the "natural" impulse frequency range for the Hodgkin-Huxley model under constant current stimulation (Fig. 5)—the dynamics begin to resemble those of the axon at the opposite end of the range of locking frequencies f_0. For the model, this dynamic response implies the presence of significant conductance perturbations as a first order response to the perturbation current component of the stimulus (see Discussion).

Dynamics of the Model Modified to Include the Effects of K^+ Accumulation in a Periaxonal Space

A modification of the Hodgkin-Huxley model which takes into account a recurrent elevation of the K^+ ion concentration at the external surface of the axolemma (due to periodic increases in K^+ membrane current as a result of impulses) as well as modified rate constants for the model state variables n and h (see Adelman and Fitzhugh, 1975 for details) was subjected to dynamic analysis for two widely separate values of I_0. The magnitudes of I_0 = 11–22 μA/cm^2 and f_0 = 88 μA/cm^2 correspond to the stimuli used to produce one-to-one phase-locking

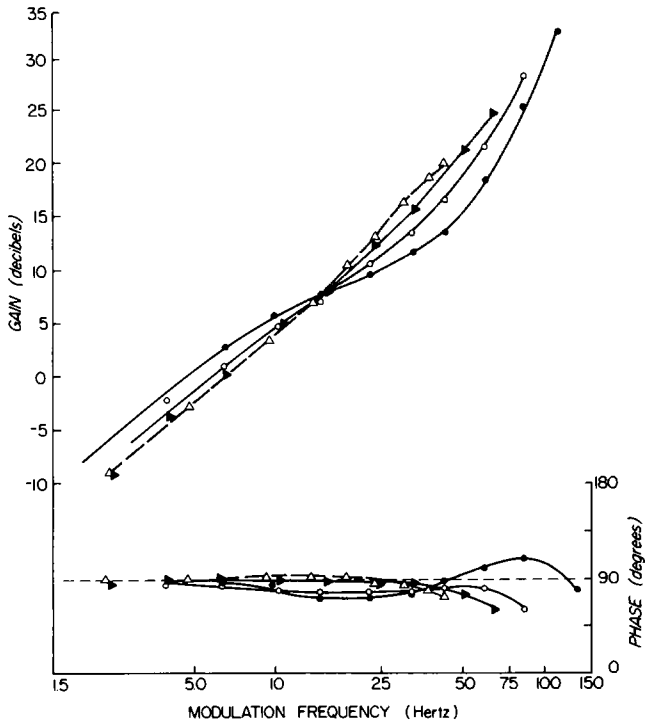

FIGURE 7 Gain and phase plots generated by the fully modified Hodgkin-Huxley model at 6.3°C. Model parameters are those of Adelman and Fitzhugh (1975, Fig. 11). The value of I_0 is 11 μA/cm^2 for $50 \leq f_0 \leq 100$ impulses/s, and 22 μA/cm^2 for f_0 = 150 impulses/s. Perturbation amplitude is 25% of I_0 for all curves ($I_1 = 0.25\ I_0$). f_0 = 150 Hz (●), 100 Hz (○), 75 Hz (▶), and 50 Hz (△).

behavior in the Hodgkin-Huxley model and the squid axon, respectively. This so-called "fully modified" model is both sufficiently sensitive to produce one-to-one phase locking for the smaller values of I_0, and sufficiently adaptive to prevent double spiking for the larger value of I_0.

Inspection of the Bode plots (Fig. 7 and 8) shows that the model dynamics are qualitatively different for the two magnitudes of I_0. For the smaller values the dynamic response resembles that of the Hodgkin-Huxley model (Fig. 6). For the larger value of $I_0 = 88\ \mu A/cm^2$ the model dynamics are superficially similar to those of the squid axon (Fig. 3). Despite such similarities there are important differences in the dynamics which will necessitate specific changes in the model.

A comparison of the dynamics of the Hodgkin-Huxley model and of the fully modified model stimulated with the smaller values of I_0 (Figs. 6 and 7) shows gain and phase curves of almost identical form with similar curves corresponding to different locking frequencies, f_0. Thus the Hodgkin-Huxley model curves for $f_0 = 75$ Hz are virtually identical to the curves for $f_0 = 100$ Hz generated by the fully modified model. Similarly, interpolating between the curves generated by the fully modified model for $f_0 = 100$ and 150 Hz shows that dynamics for $f_0 = 133$ Hz correspond to those generated by the Hodgkin-Huxley model for $f_0 = 100$ Hz.

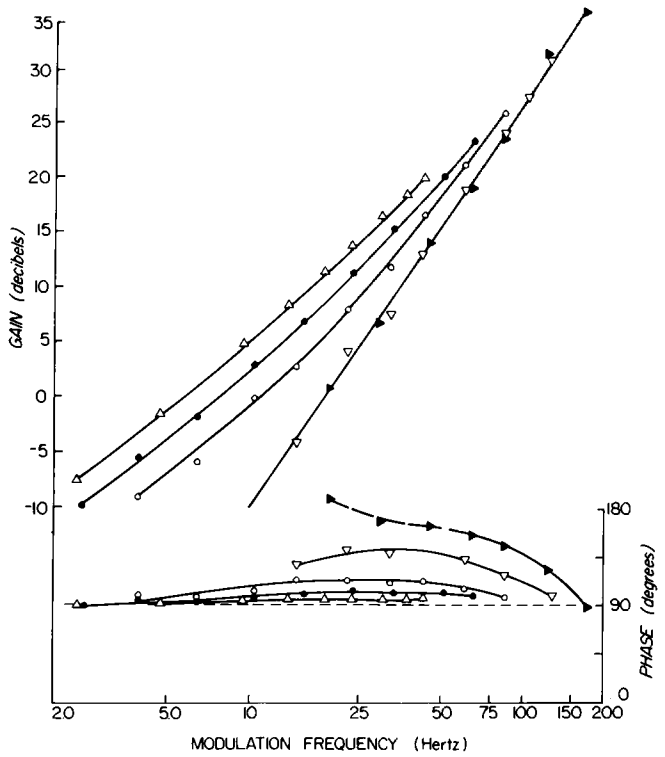

FIGURE 8 Gain and phase plots generated by the fully modified Hodgkin-Huxley model at 6.3°C with $I_0 = 88\ \mu A/cm^2$ for all values of f_0. Model parameters are from Adelman and Fitzhugh (1975, Fig. 11). Perturbation amplitude is 25% ($I_1 = 0.25I_0$). $f_0 = 200$ Hz (▶), 150 Hz (▽), 100 Hz (○), 75 Hz (●), and 50 Hz (△).

This shift in the frequency f_0 corresponding to similar dynamics is therefore ~ 33%. Both this dynamic shift and the ability of the fully modified model to phase-lock at 150 impulses/s with I_0 = 20 μA/cm^2 is a direct consequence of the relatively smaller K conductance in the interspike interval generated by this model during sinusoidal stimulation in comparison with the unmodified Hodgkin-Huxley model (see Discussion).

A comparison between axonal dynamics and those of the fully modified model stimulated with I_0 = 88 μA/cm^2 (Fig. 3 and 8) reveals the following differences: (*a*) The decline of the phase lead to well below 90° as the perturbation frequency f_m approaches, f_0, which is a general feature of the axonal dynamics, is absent in the model dynamics. (*b*) Scanning across the separate curves corresponding to separate values of the locking frequency f_0 one observes more or less abrupt changes in the dynamics occurring between certain adjacent values of f_0. For the axon this occurs between f_0 equal to 75 and 100 Hz, and for the fully modified model between 100 and 150 Hz. For the higher f_0 in each case the gain decreases dramatically at the low end of modulation frequencies f_m (towards the left side of the plots). Interspike intervals are ~10.6 ms when f_0 is 75 Hz, 7.3 ms for 100 Hz, and 4.0 ms for 150 Hz if one subtracts the width of the spike (~2.7 ms at 6.3°C) from the firing period. Large changes in the dynamics imply that the time-course of system variables during the interspike interval changes qualitatively as a function of the frequency f_0. Computed membrane conductance trajectories for the fully modified model phase-locked to f_0 = 75, 100, and 150 Hz show this feature in Fig. 9 A; B, and 10 B. Note also in frames C and D of Fig. 9 that the axonal impulse- and membrane-potential trajectory responses to locking signals of 75 and 100 Hz correspond closely to those of the model with f_0 = 100 and 150 Hz, respectively (with all systems operating at 6.3°C).

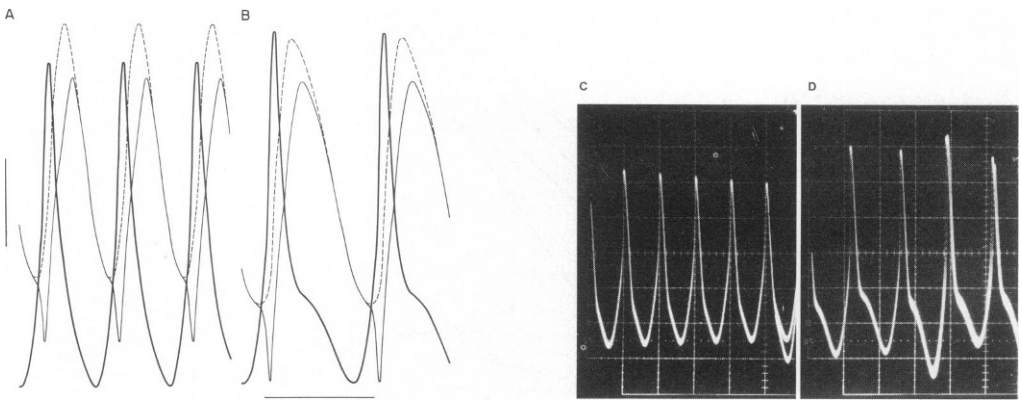

FIGURE 9 (A, B) Membrane potential (dark solid curve), g_m (defined in Eq. 3, light solid curve) and g_K (light dashed curve) generated by the fully modified Hodgkin-Huxley model at 6.3°C in response to the "locking signal" current density (Eq. 1) with I_0 = 88 μA/cm^2. Vertical bar represents units of 2 mmho/cm^2 for the conductance curves and 24 mV for membrane potential. Horizontal bar is 10 ms. (A) f_0 = 150 Hz. (B) f_0 = 100 Hz. (C, D) Oscilloscope traces of the axonal membrane potential in response to the modulated locking-current density (Eq. 2) at 6.3°C. (C) f_0 = 100 Hz. Impulse peaks are decreasing in response to the particular modulation phase present, and do not indicate a deteriorating axon. (D) f_0 = 75 Hz. Note the similarity in the membrane potential trajectories between frames A and C and between frames B and D.

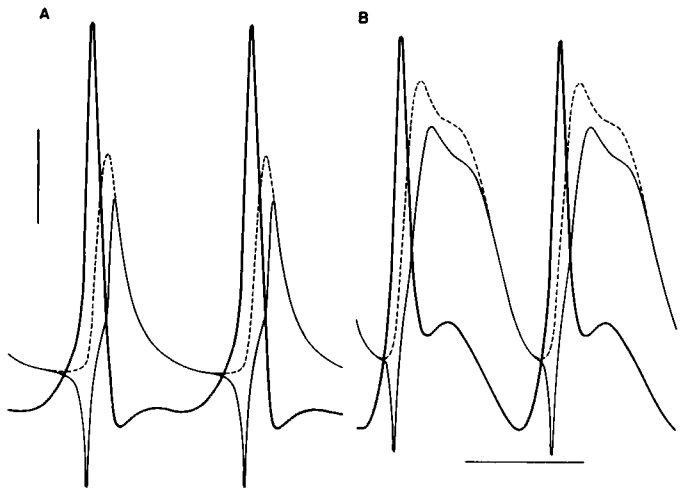

FIGURE 10 Membrane potential (dark solid curve), g_m (light solid curve) and g_K (light dashed curve) generated by the fully modified Hodgkin-Huxley model at 6.3°C in response to the locking signal current density (Eq. 1) for f_0 = 75 Hz. (A) I_0 = 11 μA/cm^2. (B) I_0 = 88 μA/cm^2. All other parameters are as in Fig. 9.

DISCUSSION

Categories of Dynamic Response

The dynamical data presented in the foregoing fall into two qualitatively different categories. The first category is characterized by a phase advance of more than 90° in the midrange of modulation frequencies and gain curves with slope everywhere $\geq$6 dB/octave, the second category with phase advances falling below 90° in the midrange with a simultaneous decrease in gain slope to <6 dB/octave. All "simple" models—those without voltage-dependent conductances and operating with a fixed, defined threshold potential (e.g., the "leaky integrator" models and the "gaussian-g_m" model of the Appendix)—fall into the second category. Such models are nonadapting and always respond with tonic repetitive firing when stimulated with an adequate constant current. They begin to break the one-to-one phase-locked condition by double spiking or missing spikes when one attempts to extrapolate to locking frequency and stimulus conditions which "should" otherwise produce a midrange phase increase and direct steepening of the gain slope.

The Hodgkin-Huxley model, when "locked" to an impulse frequency >55 Hz by an adequate stimulus also produces dynamics of the second category. This range of impulse frequencies (above 55 Hz) is also the range of repetitive firing for the model when stimulated with constant current (Fig. 5). The cumulative evidence on repetitively firing systems therefore points to the tentative conclusion that all such systems produce dynamic responses that fall into the second category.

The inverse statement that second category dynamics imply a repetitively firing model is not true as shown by the dynamics of the fully modified model in Fig. 7. It is true, however, that the model is more oscillatory in response to a current step to 22 μA/cm^2 as shown by the

generation of a second partial spike which is absent for a step to 88 $\mu A/cm^2$ (Adelman and Fitzhugh, 1975, Fig. 11). The dynamics appear to recognize this trend to impending repetitive activity.

Repetitively firing systems and the second category in general are characterized by the absence of dynamic phenomena which, if present, would completely obscure those indications of a corner frequency which are definitive of the second category. There exist, however, strongly adapting systems that are either capable of producing (the fully modified model) or invariably produce (the squid axon membrane) a dynamic response of the first category. Such a response may be interpreted as the total obscuration of the corner frequency by dynamic phenomena which are not necessarily related to the resonance. Instead, these additional phenomena are first order dynamic responses to a stimulus-induced modulation of conductance parameters.

Membrane Conductance Perturbations and Summing Phenomena

For the leaky integrator model (see Appendix) both the corner frequency and the resonance width increase when the model membrane conductance g_m is increased. In fact, the corner frequency equals $g_m/2\pi C_m$. For the more complex models we define the conductance:

$$g_m(E, t) \stackrel{\text{def}}{=} g_K(E, t) + g_{Na}(E, t) \left\{ \frac{E - E_{Na}}{E - E_K(I_K, t)} \right\}. \tag{3}$$

This conductance, g_m, simply casts the equation,

$$C_m \dot{E} = - g_K(E, t) \{E - E_K(I_K, t)\} - g_{Na}(E, t) \{E - E_{Na}\} + I, \tag{4}$$

into the form of the leaky integrator Eq. A4 with time-varying and voltage-dependent g_m and E_K according to the particular complex model to be analyzed. (E_K varies only according to changes in periaxonal space K^+ concentration.) The conductance, g_m, is the proportionality "constant" relating the ionic (noncapacitative) portion of the membrane current to membrane potential referenced to E_K: $g_m = (I_{Na} + I_K)/(E - E_K)$. g_{Na} and g_K are true electrical conductances; however, the final term in Eq. 3 acts as a negative conductance which leads to the regenerative properties of the membrane potential during the rising phase of action potentials.

Because the locking signal is stereotyped the conductance time-course may be determined and, when not perturbed by I_1, is a function only of I_0 and f_0 for a given model. The conductance time-courses of unperturbed, phase-locked impulse trains generated by the "fully modified" model are shown in Fig. 10 for I_0 = 11 and 88 $\mu A/cm^2$ and f_0 = 75 Hz. Note the elevated conductance until just before an impulse with I_0 = 88 $\mu A/cm^2$. This conductance elevation late in the interval is the result of the stimulus current as compared to the naturally generated early conductance peak as a part of the impulse response (Fig. 10 A).

Consider first the case of the just adequate stimulus, I_0 in the approximate range of 10–22 mA/cm^2. For a given complex model showing dynamics of the second category the resonance width in the gain increases as the locking frequency f_0 is increased. This may be seen by shifting the curves in Fig. 6 and 7 horizontally to superimpose the values of f_0 (in Fig. 6 only for f_0 = 75 and 100 Hz). Furthermore, the high f_m phase bulges to a greater advance for higher f_0. As f_0 increases, both the average conductance level increases and each impulse

occurs nearer to the foregoing conductance peak. These dynamic changes agree completely with those of simple models when their conductance parameters are changed (cf. Appendix Fig. 13). They strongly suggest that conductance perturbations as a result of the presence of the "small amplitude" modulating sine wave are insufficient to be recognized to first order in the dynamics, and are therefore likely to be small.

Consider next the case of the fully modified model driven with $I_0 = 88\ \mu A/cm^2$ (Fig. 10). Although the conductance level is high throughout the interspike interval as an indirect result of the large current, the phase enhancement in the midrange of f_m and the direct steepening of the gain curve cannot be attributed simply to an increase in resonance width. As shown by the dynamic response of the gaussian-g_m model in the Appendix (Fig. 13), an elevated conductance is not sufficient by itself to generate dynamics of the first category. The midrange phase and gain increase however are a natural signature of certain summing phenomena which include summing (recurrent) inhibition (Fohlmeister et al., 1977*a*) and summing conductance increases (Fohlmeister, 1979). Summing in this context means that an impulse does not reset the pertinent state variables to fixed initial conditions at the beginning of each interspike interval, but in effect adds an amount to the value just before the impulse. The variable subsequently relaxes. The mean value of the summing variable changes from interval to interval because its level is frequency dependent and frequency is modulated.

Summing phenomena- and stimulus-induced conductance modulations, when present, both lead to periodically varying conductance levels. ("Conductance level" may be defined as the conductance at a fixed time, say 5 ms, after each impulse which is updated in each interval.) We will argue in the following that both types of phenomena are probably present in varying degree for both the axon and complex models when they exhibit first category dynamics. A difference between the action of a summing variable and a stimulus-induced modulation lies in the phase relationship of the phenomenon to the modulating stimulus sine wave: the summing peak will occur at the times of peak impulse frequency whereas a stimulus-induced modulation will follow the phase of the modulating current. However, it appears that this phase difference in the conductance modulation is unimportant to the generation of first category dynamics. Because it is impossible to derive closed form mathematical expressions for the transfer function (gain and phase) of complex models, the following discussion is based on what is known from the dynamic behavior of a summing variable in the context of simple models. The perturbation frequency, f_m, at which the phase peak occurs is a function of the relaxation time of the summing variable (Fohlmeister et al., 1977*a*, Fig. 7) in such a way that a shorter time constant corresponds to a higher peak frequency, f_m. Note that the phase peak for the fully modified model firing at $f_0 = 150$ Hz (Fig. 8) occurs at $\sim f_m = 35$ Hz and for the axon for $f_0 = 75$ and 100 Hz (Fig. 3) in the range of $f_m = 15$–20 Hz. The relaxation time of the summing variable is ~2.5 ms for a phase peak of 35 Hz and ~5 ms for a peak at 18 Hz. These times are in the range of relaxation times of the K conductance and the Na-inactivation parameter h, and therefore suggest that additional processes with longer relaxation times may be operating in these membrane subsystems. The degree to which anomalous sodium channel inactivation effects (see Jakobsson, 1978 for references) or a slower K-channel process might affect the dynamics awaits further analysis.

Consider now the question of a summing phenomenon-vs. stimulus-induced conductance modulations. Following the onset of a locking signal of the form $I(t) = I_0(1 - \cos 2\pi f_0 t)$

applied to the axon with f_0 = 100 Hz and the fully modified model with I_0 = 88 μA/cm^2 and f_0 = 150 Hz we noted a transient decrease in spike height with a duration of at least four impulses, and no adjustment of the impulse locking phase after the first impulse. This spike height transient is evidence for an impulse-induced perturbation of conductance parameters with the property that the parameters are reset to values that depend on the state before the impulse, a state that is changing throughout the transient. This behavior indicates the presence of a significant summing phenonemon in these cases. Stimulus-induced conductance modulations are probably the dominant cause for most other cases of first category dynamics shown in this report. For the Hodgkin-Huxley model phase-locked to f_0 = 25 Hz, the phase peak at $f_m \doteq 7.5$ Hz (Fig. 6) is unlikely to be the result of a summing phenomenon. The interspike interval is simply too long in relation to the relaxation times of all model state variables for any significant "memory" of the state in previous intervals. Indeed, no such memory is indicated by the dynamic response of the model at higher f_0 for which the required memory would be shorter and which is of the second category.

A similar conclusion holds also for the dynamic response of the fully modified model stimulated with I_0 = 88 μA/cm^2 at locking frequencies $f_0 < 100$ Hz. The spike height transient noted for f_0 = 150 Hz is largely absent for the lower locking frequencies. On the other hand significant conductance level changes as a result of the modulating sine wave itself may be inferred from the spike height modulation which is entirely in phase with the stimulus (Fig. 2 A).

Finally, the fully modified Hodgkin-Huxley model operates with an implicit summing variable, E_K, as a logarithmic function of K_s, the K^+ concentration in the periaxonal space. K_s is periodically elevated above the value just before each spike by the K^+ current associated with the impulse. Bode plots were obtained with conductance channel rate constants of the fully modified equations with I_0 = 88 μA/cm^2, but holding K_s fixed at 12 meq. These plots did not show any significant changes in the quality of the fully modified model dynamics. It follows that the summing properties of the variable K_s are not responsible for the first category dynamics of this model; its influence is sufficiently indirect so as not to generate a specific signature in first order dynamics.

Dynamic Response to Adequate and Excessive Stimulation

A model driven with a just adequate stimulus shows the greatest amount of structure in gain and phase whereas an excessive stimulus results in a "stiffening" of the dynamic response. This stiffening is clearly seen in the model phase curves which tend to flatten throughout the range of values of f_m (Fig. 8). Dynamic analysis therefore is richer in information when carried out with a just adequate stimulus.

An important feature of the axon's phase—which is not shared by the fully modified model when stimulated with the "excessive" value of I_0 = 88 μA/cm^2—is the decline in phase advance to well below 90° for f_m in the vicinity of f_0. This decline in phase which occurs for all values of f_0 for the axon may be related to a relatively high threshold in relation to the stimulus magnitude I_0. Note that all model systems driven with a just adequate stimulus show a similar phase decline (Fig. 6 and 7) whereas when stimulated with an excessive value of I_0 the phase advance remains >90° as $f_m \rightarrow f_0$ (Fig. 8). Bringing the levels of adequate stimulus into line is therefore considered necessary for further model development based on dynamic analysis.

The authors acknowledge the assistance of Clyde Tyndale and Richard Waltz for the development of the data acquisition system at the Marine Biological Laboratory.

Research supported in part by National Science Foundation grants BNS 77-22532, PCM 78-25168 and U.S. Public Health Service grant EY 00293 to the University of Minnesota. Computer Facilities were made available in part by the Air Force Office of Scientific Research (AFOSR—1221) and by the University of Minnesota Computer Center.

Received for publication 25 May 1979 and in revised form 12 December 1979.

APPENDIX

A statistical analysis of nerve-impulse trains produced by sinusoidally modulated current stimuli has been used in connection with certain well-defined models to describe the behavior of membrane properties in the interspike interval (see Fohlmeister et al., 1977*a*, for references). In this section we will summarize the basic approach and the important results of previous studies employing the approach that are applicable to the squid axon preparation.

A train of action potentials can be induced in a *repetitively firing* neuron by a constant depolarizing current, I_0 ($a = 0$ in Eq. 1), or by a sinusoidal current having a frequency equal to the impulse repetition rate, f_0 (Eq. 1). For the second type of stimulus, the amplitude of the sinusoid (equal to aI_0 in Eq. 1) must be sufficiently large so that the impulse repetition rate follows the sinusoidal frequency when the latter is changed within a neighborhood of f_0—that is, the impulses must be phase-locked to the stimulus sinusoid (Fig. 1). The two methods of producing a repetitive discharge are not equivalent dynamically and may lead to different measures of membrane properties. In both cases, calculations are made from measured impulse occurrence times when the steady-state repetitive discharge is modulated by adding to the stimulus current a sinusoidal perturbation with frequency $f_m < f_0$ and of small magnitude so that the modulation is of the order of 10–25%. When the unperturbed stimulus is as in Eq. 1, the total stimulus current density then has the form

$$I(t) = I_0\{1 + a \cdot \sin(2\pi f_0 t)\} + I_1 \sin(2\pi f_m t + \varphi) \tag{A1}$$

of which Eq. 2 is a special case with $a = 1.0$ (φ is an arbitrary phase angle).

Estimates of impulse density over a single perturbation cycle are made at a number of different perturbation frequencies (see Fohlmeister et al., 1977*a* for details about methods of estimating impulse density). The amplitude, A, of the modulation is defined as one-half the total change in impulse density over a single cycle. This value is converted into a "gain" in decibels, where

$$\text{Gain} \overset{\text{def}}{=} 20 \log_{10} kA \tag{A2}$$

The constant k has a value of 1 with units of $(\text{amplitude})^{-1}$. The phase of the impulse density is determined with respect to the modulating sinusoid and is given in degrees of lead (+) or lag (−). Gain and phase are plotted as functions of log modulation frequency, f_m, to form Bode plots. Those plots show certain features that relate specifically to the membrane parameter

$$\gamma \overset{\text{def}}{=} g_m / C_m \tag{A3}$$

for the interspike interval. Based on previous studies of models and sensory neurons we have made the following interpretations of the Bode plot curves.

Sinusoidal Perturbation of a Constant Stimulus

Consider first the case in which a tonic repetitive activity is induced by a constant current ($a = 0$ in Eq. A1). A typical Bode plot is illustrated in Fig. 11. The gain curve is flat for low modulation frequencies up to at least $(0.1)f_0$. For higher frequencies, the gain increases, approaching a resonance peak at $f_m = f_0$.

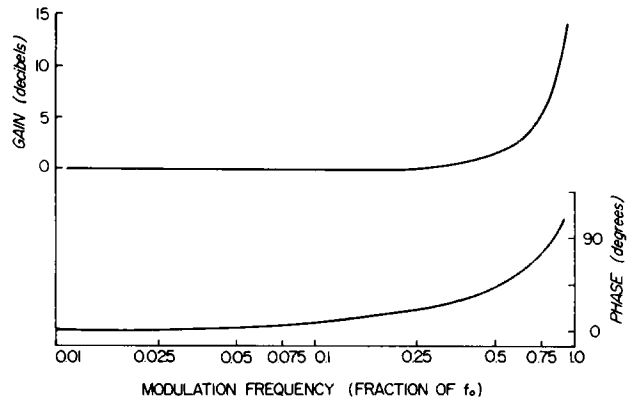

FIGURE 11 Gain and phase for a typical case of tonic repetitive activity induced by constant current. Curves are calculated from the analytical solution for a repetitively firing model (Fohlmeister et al., 1977*a*) for $\bar{\gamma}/f_0 = 3.0$.

The half-width of the resonance depends both on a weighted mean value of γ in the interspike interval designated $\bar{\gamma}$ and on the value of f_0 such that a given curve is completely defined by $\bar{\gamma}/f_0$. Thus, the value of $\bar{\gamma}$ is determined from the gain curve by fitting it to calculated curves for known values of $\bar{\gamma}/f_0$ as shown below. In the case of Fig. 11 the resonance corresponds to $\bar{\gamma}/f_0 = 3$. Lower values will lead to narrower resonances and reduced phase shifts.

The phase curve depends further on the time-course of $\gamma(t)$ in the interspike interval although its general features always include a phase lead that increases with increasing modulation frequency. The phase curve is useful in testing specific hypotheses about the temporal structure of $\gamma(t)$ but not in determining a value of $\bar{\gamma}$. In general the phase lead for high f_m is small when γ is large only very early in the interval, and increases when γ is weighted more heavily later in the interval.

Sinusoidal Perturbation of the Locking Sinusoidal Stimulus

The second case to consider is the one in which a repetitive activity is induced by sinusoidal current stimulation at the frequency f_0. The conditions necessary for one-to-one phase locking are discussed in Rescigno et al. (1970) and Poppele and Chen (1972). The modulation is provided by the second sinusoid of Eq. A1, and the impulse train is analyzed with respect to this sinusoid. Because the type of modulation is different in this case, pulse position modulation instead of pulse frequency modulation, the Bode plot gives an entirely different gain and phase behavior (Fig. 12) which is, however, superimposed on the behavior described in the preceeding subsection.

The gain curve increases with a slope of 6 dB/octave to a "corner frequency" at $f_m = \omega_0/2\pi$. At that frequency the gain is 3 dB down from the flat gain level at the higher frequencies (see dashed curves in Fig. 12). The phase is $+90°$ at the lowest modulation frequencies and it shifts toward 0° at the higher frequencies (note dashed phase curves in Fig. 12). The phase equals $+45°$ at the "corner frequency" $f_m = \omega_0/2\pi$. Note that these features are obscured more or less by the addition of the resonance behavior observed in Fig. 11. The degree of interaction depends on the values of f_0 and ω_0 that apply in a particular case.

Effect of Model Parameters on Bode signatures

As suggested in the above sections, the parameter γ determines many features of the Bode signature. Models employing a constant γ (i.e. a constant conductance g_m) in the interspike interval, referred to as "leaky integrator" models, follow the linear equation for E in the interspike interval:

$$\dot{E} = -\gamma(E - E_K) + I/C_M \qquad \text{(A4)}$$

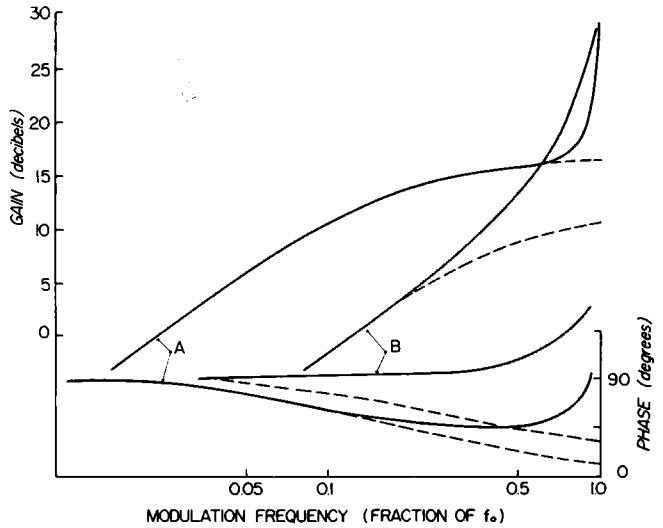

FIGURE 12 Gain and phase for a typical case of tonic repetitive activity induced by a locking sinusoidal current. (A) Calculated for $\bar{\gamma}/f_0 = 1.0$ and showing a clear separation between the corner frequency and resonance. (B) Calculated for $\bar{\gamma}/f_0 = 3.0$ such that f_0 is less than the minimum stable firing rate for the model with constant current stimulation; (note Fig. 5). In this case the corner frequency is no longer apparent. Dashed curves represent the corresponding dynamics with the resonance subtracted out showing the corner frequencies clearly.

This equation is supplemented with threshold and reset conditions (fixed values of E) to produce impulse trains. The leaky integrator is used to calibrate the resonance width at $f_m \rightarrow f_0$. The $\bar{\gamma}$ of any more general model is simply defined to be equal to the particular value of γ of the leaky integrator model which generates the same resonance width in the gain. Thus, $\bar{\gamma} = \gamma$ for the leaky integrator by definition.

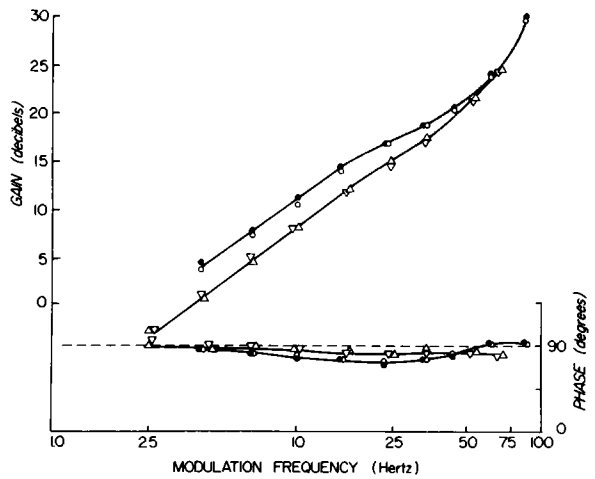

FIGURE 13 Gain and phase plots generated by the simple gaussian-g_m model for $f_0 = 100$ Hz (●, ○) and 75 Hz (▽, △). Parameters are $g_0 = 0.25$, $g_1 = 6.5$ mmho/cm^2, $t' = 3.0$ ms and $\sigma = 8.165$ ms for (●, ▽) and $g_0 = 0.25$, $g_1 = 5.0$ mmho/cm^2, $t' = 5.0$ ms and $\sigma = 6.742$ ms for (○, △).

The value of ω_0 has been shown to be equal to the value of γ for these models. It therefore follows that $\bar{\gamma} = \omega_0$ for this case. For more complex models we define $\gamma_e \equiv \omega_0$ to be the "equivalent γ". In general γ_e (as well as $\bar{\gamma}$) is a function of f_0 for complex models. When $\gamma(t)$ is not constant, $\bar{\gamma} \neq \gamma_e$ in general (Fohlmeister et al., 1974).

The leaky integrator is a special case of a more general class of models for which $\gamma(t)$ is defined to be a specific function only of the time since the last impulse. Members of this class, which are called "simple models" in this report, are distinguished by the condition that $\gamma(t)$ is independent of (not a function of) membrane potential or stimulus current except for the establishment of its initial value, $\gamma(0)$, in each interspike interval. As a nontrivial example of this class of models—one which is referred to in the discussion section—we have analyzed the dynamic response of the gaussian-g_m model for which

$$g_m(t) = g_0 + g_1 e^{-(t-t')^2/\sigma^2} \tag{A5}$$

For this model $\gamma(t)$ peaks at time t' milliseconds after each impulse, but is otherwise independent of the stimulus or membrane potential. The dynamics of this model were determined for the case of the locking stimulus for impulse frequencies, f_0, pertinent to the squid axon (Fig. 13). The importance of these plots derives from the recognition that the resonance width is not so large as to completely obscure indications of a corner frequency despite the large conductance in the midrange of the interspike intervals. In this respect the model agrees with the dynamics of the leaky integrator (cf. Fig. 12 A).

The presence of a process that can accumulate or summate from one interval to the next leads to adaptive behavior, which also provides a characteristic signature in the Bode plot that is further superimposed on the behavior already described. This can be illustrated by referring to the example of a negative feedback that results from a hyperpolarizing current generated in response to an action potential (Fohlmeister et al., 1977*b*). In that example, a current of magnitude I_h is induced after each spike and then decays with time constant τ. As long as the charge $I_h \cdot \tau$ is sufficiently large so that a significant fraction of the current continues to flow at the end of the interspike interval, that fraction is added to the current I_h induced by the succeeding spike. Because the current is hyperpolarizing, the effect is to produce successive lengthenings of the interspike interval. The signature of this kind of adaptation in the Bode plot is illustrated in Fig. 14. The magnitude of the effect depends on the ratio I_h/I_1 (Fohlmeister et al., 1977*a*, Results); for a given f_0, its frequency response depends on the value of τ (Fohlmeister et al., 1977*a*; Fig. 7). There is a phase advance for $f_m < f_0/2$ and a phase lag for $f_0/2 < f_m < f_0$. The gain is highest at $f_m = f_0/2$ being reduced at the low and high frequencies in the interval $(0, f_0)$. These features in the Bode plot are produced by any process leading to the functional equivalent (adaptation) of the summating negative feedback described above. They may involve accumulating conductance changes (Fohlmeister, 1979) or additive changes in threshold, for example. Fig. 15 shows how the adaptive behavior further modifies the Bode signatures induced by γ. In this case the effects shown in Fig. 14 are added to the Bode signatures of a leaky integrator model in which repetitive firing was induced by a locking signal (Fig. 12 B).

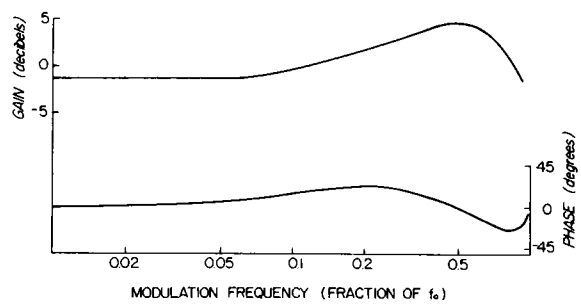

FIGURE 14 Isolated gain and phase components associated with adaptation for which $I_h/I_1 = 0.4$, $\tau = 4.5$ ms and $f_0 = 100$ Hz.

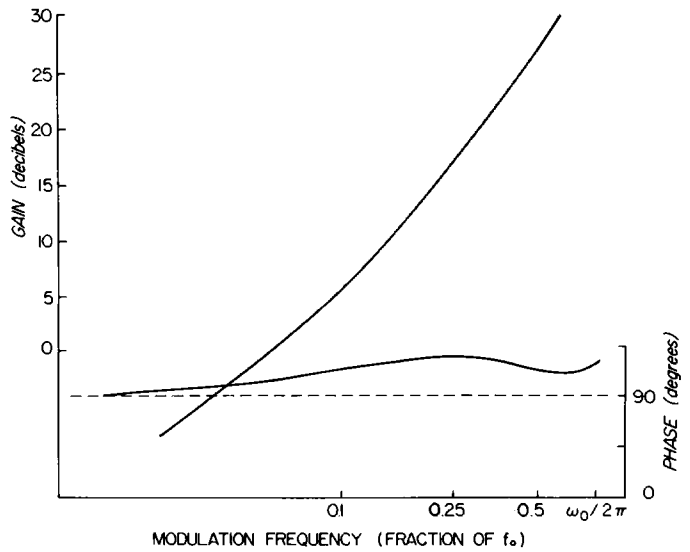

FIGURE 15 Gain and phase for a typical case of tonic repetitive activity of a model in which adaptation as in Fig. 14 has been added to the model response illustrated in Fig. 12 B.

REFERENCES

ADELMAN, W. J., and R. FITZHUGH. 1975. Solutions of the Hodgkin-Huxley equations modified for potassium accumulation in a periaxonal space. *Fed. Proc.* **34**:1322–1329.

ADELMAN, W. J., Y. PALTI, and J. SENFT. 1973. Potassium ion accumulation in a periaxonal space and its effect on the measurement of membrane potassium ion conductance. *J. Membr. Biol.* **13**:387–410.

BEST, E. N. 1979. Null space in the Hodgkin-Huxley equations. *Biophys. J.* **27**:87–104.

BINSTOCK, L., W. J. ADELMAN, J. P. SENFT, and H. LECAR. 1975. Determination of the resistance in series with membranes of giant axons. *J. Membr. Biol.* **21**:25–47.

FOHLMEISTER, J. F. 1975. Adaptation and accommodation in the squid axon. *Biol. Cybern.* **18**:49–60.

FOHLMEISTER, J. F. 1979. A theoretical study of neural adaptation and transient responses due to inhibitory feedback. *Bull. Math. Biol.* **41**:257–282.

FOHLMEISTER, J. F., R. E. POPPELE, and R. L. PURPLE. 1974. Repetitive firing: dynamic behavior of sensory neurons reconciled with a quantitative model. *J. Neurophysiol.* **37**:1213–1227.

FOHLMEISTER, J. F., R. E. POPPELE, and R. L. PURPLE. 1977*a*. Repetitive firing: a quantitative study of feedback in model encoders. *J. Gen. Physiol.* **69**:815–848.

FOHLMEISTER, J. F., R. E. POPPELE, and R. L. PURPLE. 1977*b*. Repetitve firing; quantitative analysis of encoder behavior of slowly adapting stretch receptor of crayfish and eccentric cell of *Limulus*. *J. Gen. Physiol.* **69**:849–877.

GUTTMAN, R., and L. FELDMAN. 1978. Frequency entrainment of squid axon membrane. *Biophys. J.* **21**:83*a*. (Abstr.)

HAGIWARA, S., and Y. OOMURA. 1958. The critical depolarization for the spike in the squid giant axon. *Jpn. J. Physiol.* **8**:234–239.

HODGKIN, A. L., and A. F. HUXLEY. 1952. A quantitative description of membrane current and its application to conduction and excitation in nerve. *J. Physiol. (Lond.).* **117**:500–544.

HOLDEN, A. V. 1976. The response of excitable membrane models to a cyclic input. *Biol. Cybern.* **21**:1–7.

JAKOBSSON, E. 1978. A fully coupled transient excited state model for the sodium channel. *J. Math. Biol.* **6**:235–248.

POPPELE, R. E., and W. CHEN. 1972. Repetitive firing behavior of mammalian muscle spindles. *J. Neurophysiol.* **35**:357–364.

RESCIGNO, A., R. B. STEIN, R. E. POPPELE, and R. L. PURPLE. 1970. A neuronal model for discharge patterns produced by cyclic inputs. *Bull. Math. Biophys.* **32**:337–353.